16th World Conference on Earthquake, 16WCEE 2017

Santiago Chile, January 9th to 13th 2017

Paper N° 2372 (Abstract ID)

Registration Code: S-O1477550314

Development of Seismic Fragility Curves of Horizontal Curved Bridge Using Neural Network Prediction

K. Karimi-Moridani [(1)], P. Zarfam [(2)]

[(1)] *PhD Candidate, Department of Structural Engineering, Science and Research Branch, Islamic Azad University, Tehran, Iran, karimi.k@srbiau.ac.ir*

[(2)] *Assistant Professor, Department of Structural Engineering, Science and Research Branch, Islamic Azad University, Tehran, Iran, zarfam@srbiau.ac.ir*

Abstract

In this study a Soft Computing approach for the seismic fragility assessment of horizontal curved bridge is developed. In recent years, seismic fragility curves are often determined by using analytical method in structures. In order to build neural network structure, Nonlinear time history analysis is performed by 129 natural records in OpenSees. This records have been chosen from the PEER strong motion database and scaled on 0.1g to 1.3g. The structure of the neural network is based on input ground motions and output of nonlinear dynamic analyses of bridge. Arias Intensity, cumulative absolute velocity, characteristic intensity and specific energy density reflect the amplitude, the duration of a strong ground motion, the frequency content and energy respectively, and they correlate well with structural damage. Kolmogorov-Smirnov and Shapiro-Wilk tests was performed to normalize the data. Approach to reducing the computational effort in the evaluation of fragility, a neural network was considered in this study, which can provide accurate predictions of the structural response. The proposed approach is applied for bridge and a reduction of magnitude is achieved in the computational effort.

Keywords: nerual network; statistical distribution; fragility curve; bridge

1. Introduction

There are different methods of structural analysis. These methods are based on sophisticated scientific methods. Structural analysis methods based on mechanical principles theory, computational methods and results analysis obtain through the discrete numerical simulation. Moreover, heuristic methods have been proposed in recent decades compared with the results of computational methods are reliable. Recently, many studies of the computational methods such as neural networks and fuzzy logic are used in various fields of engineering. The use of which has been a growing trend in recent decades. There have many studies led to the fragility curves. Seismic vulnerability assessment can be expressed through fragility curve. Also, these curves demonstrate the need for retrofitting and the effect of the structural components in crisis management. Generation of curves to empirical methods, analytical and heuristic can be derived.

Mander studies led to fragility curves that were used to determine the seismic vulnerability of highway bridges. In comparison with experimental methods, this method improved the reliability factor of fragility curves [1]. Sang et al. stated the analysis results of fragility in highway bridges under earthquake with regards to spatial variation. Their study illustrated the fragility is underestimated in cases that the bridges are analyzed by similar excitations in comparison to when it is Dissimilar [2]. Yamazaki et al. Stated the effects of isolation the structure onto the fragility curves in a simple approach [3]. The studies of Hoom Kim et al. declared improvement in fragility after retrofitting [4]. The Nielson et al. works led to fragility curves of different types of highway bridges [5]. Padget and Destreches presented a methodology for finding fragility curves of retrofitted bridges and achieved the improvement in fragility [6]. Studies of CarloMarano and et al. is Analytical evaluating of essential facilities fragility curves by using a stochastic approach [7]. Mitropoulou et al. provided fragility curves of regular and irregular structures based on neural networks and illustrated the fragility results are very appropriate using a neural network approach. The methodology is based on the assumption that demand values follow the lognormal distribution; thus, fragility curves in lognormal distribution are expressed in two parameters (mean and standard deviation) [8]. Rajeev et al. demonstrated that seismic vulnerability of reinforced concrete structures with irregular consideration [9]. The derivation of state-dependent fragility curves for masonry buildings by analytical method used in Penna et al. work [10]. Goda et al. Handle Incremental dynamic analysis of wooden structures and effect of dominant earthquake scenarios on seismic fragility [11]. Hancilar et al. provided the fragility of probabilistic analysis in school buildings by using common analytical methods [12].

Siquera et al. presented fragility curves for isolated bridges in eastern Canada using data from experimental results [13]. Fragility analysis of skewed bridges in The Southeast of the US has indicate in Yang et al. Research [14]. It was observed, with the exception of reference [8] a limited number of studies have provided fragility curves using neural networks to reduce computational efforts.

2. Fragility assessment

Seismic fragility curves can be expressed using two-parameter lognormal distribution functions. These parameters are median and lognormal standard deviation, which are used to evaluate fragility as a function of the intensity measure, and the estimation of these parameters is achieved using maximum likelihood estimation [8]. The lognormal model is the most widely utilized. A brief description of likelihood function is introduced the following form :

$$\mathcal{L}\,(\mu_1, \mu_2, \ldots, \mu_n, \beta_1, \beta_2, \ldots, \beta_n) = \prod_{i=1}^{N} \prod_{j=1}^{n} F_R(IM_i\,, y_j)^{x_{ij}} \tag{1}$$

here F_R is defined as a fragility function (cumulative distribution function) for a specific state of damage, IM_i is the intensity measure. If the i-th realization of the structure sustains the state of damage under IM_ithen x_{ij} is equal to 1 otherwise its zero. The total number of structural realizations after the earthquake by N and the total number of the limit states is assigned to n. Therefore, F_R Is written as follows :

$$F_R(IM) = \Phi\left[\frac{\ln(IM|\mu_j)}{\beta_j}\right] \tag{2}$$

where $\Phi(\cdot)$ commonly denotes the standard normal cumulative distribution function. μ_j , β_j the median and logarithmic standard deviation of the fragility curve for jth damage state, respectively. By applying the harmony search optimization algorithm in the next section acheive the two parameters μ and β of Eq. (1) that maximize ln($\mathcal{L}$). The median is the quantity that has 50% probability of not being exceeded.

2.1 Incremental Dynamic Analysis

The incremental dynamic analysis (IDA) approach is a parametric analysis method that can provide a clear expression of the relationship between the demand and the seismic capacity of the structure (Fig.1). It involves performing nonlinear dynamic analyzes of a structural model under a suite of ground motion records, each scaled to several IMs. Selecting the IM and engineering demand parameter (EDP) is one of the most important steps of the IDA methodology. PEER record ground motion was adopted in this study [16]. To perform a nonlinear dynamic analysis of the bridge, a set of ground motion records is required whose characteristics are consistent with the type of fault, magnitude, soil conditions and Distance from the site. In this current work, is used 129 ground motion records to analyze horizontal curved bridge to provide sufficient accuracy of seismic demands. In the work by researchers [4, 5, 6], the EDPs in bridges are classified into three categories based on the ductility of piers, bearings, and abutment deformation.

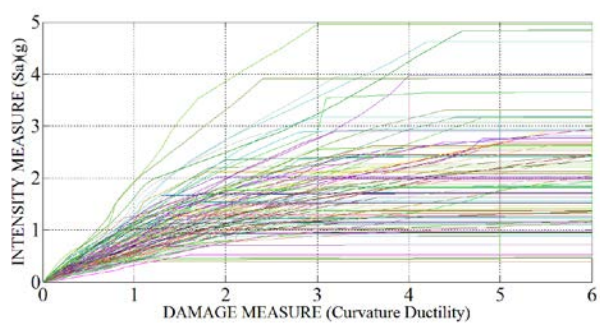

Fig. 1 –IDA curves

2.2 Optimization algorithm

In order to achieve " maximum benefit with minimum cost" we usually depend on optimization techniques. For achieving this goal, the Harmony Search (HS) algorithm is proposed and apply to solve the optimization problem [8]. A lot of problems in different scientific fields are formulated as optimization problems and solved using different optimization algorithms. The development and application of optimization models have attracted increasing attention among researchers in the last decade. The Essential parameters of these algorithm are harmony memory considering rate (HMCR) and pitch adjusting rate (PAR) which control the component of solutions and also affect convergence rate. HMS and BW are harmony memory size and bandwidth respectively. "n" is used for assigning the number of pairs of decision variables (equivalent to the number of music instruments), an HM with the size of HMS can be defined as :

$$\text{HM}=\begin{bmatrix} x_1^1 & x_2^1 & x_2^1 & \dots & x_n^1 \\ x_1^2 & x_2^2 & x_2^2 & \dots & x_n^2 \\ \dots & \dots & \dots & & \dots \\ x_1^{HMS} & x_2^{HMS} & x_3^{HMS} & \dots & x_n^{HMS} \end{bmatrix} \tag{3}$$

where $[x_1^i, x_2^i, \dots x_n^i]$ (i=1,2,…,HMS) is a solution position. HMS is typically set to be between 50 and 100. where the HMCR is the probability of selecting a component from the significant components stored in the HM and 1-HMCR is, therefore, the probability of creating HM randomly. In order to Improvise a new solution $[x_1', x_2', \dots x_n']$ from the HM, each element of this vector solution, x_j' is achieved based on the HMCR. The PAR determines the probability of a position from the HM to be grew. It should be noted, the generation of new solutions in the HS method causes full use of all the HM members, while algorithms such as genetic algorithms,generates fresh chromosomes using a maximum existing ones. With this approach, the new solution is evaluated. In this situation, If it is successful, a better fitness solution than that of the worst member in the HM, it will replace that one. Otherwise, it is eliminated. This process is repeated until a preset termination criterion, e.g., the maximal number of iterations, is reached.

3. Artificial neural networks

Artificial neural networks (ANNs) are family of biologically-inspired models (generally, the human brain), since they are composed of elements that perform in a manner analogous to the elementary functions of a biological neuron. In neural networks, a number of elements (neurons) with strong internal communications are coordinated to work together to solve problems. Processing empirical data, artificial neural networks transfer the knowledge or rules hidden in the data to the network structure, an action called learning. Basically, the ability to learn is the most important feature of a smart system. Through programming, a data structure called "node" is designed in such networks which can act like a neuron. In a neural network, nodes have two modes: active and passive and each edge has a weight. An artificial neural network is comprised of components, layers and weights. The behavior of a network is dependent on the communication between its members. Generally, there are three layers in neural networks: input, hidden, and output. The input layer includes raw information and the performance of a hidden layers is determined by inputs and the weight of connections between them and hidden layers. The performance of a output layer is related to the hidden unit activities and the weight of connections between hidden unit and output. By creating a network of these nodes and applying a training algorithm to it, the network can be trained. Despite the different neural networks, Multilayer neural networks can be used to learn nonlinear problems and problems involving various decisions. A backpropagation training set network includes n input-target pairs $\mathbf{P} = [\mathbf{I^D}, \ \mathbf{t^D}]$. If a set of weight parameters like w is allocated to network connections, a pattern like $\mathbf{t}(\mathbf{I^D}, \mathbf{W}, \mathbf{A})$ is defined between the input vector I^D and the output vector t [15] . The quality of this pattern is measured using the following error function. To use this descending gradient method, the output error must be calculated in Eq. (4) :

$$E(\overrightarrow{W}) \equiv \frac{1}{2}\sum_{d\in D}\sum_{k\in output}(t_{kd} - o_{kd})^2 \tag{4}$$

$E(\vec{W})$ is the total output error, D is the set of training samples, Outputs is the total training outputs, t_{kd} is the k^{th} value of the objective function (corresponding to the k^{th} output unit) for the d^{th} training sample, and o_{kd} is the k^{th} output value (corresponding to the k^{th} output unit) for the d^{th} training sample. Therefore, minimum iteration period of an algorithms are used to obtain the optimal values of W weight parameters [15]. Most of the numerical minimization methods are based on the following form :

$$W^{(s+1)} = O(W^{(s)}) = W^{(s)} + \Delta W^{(s)} \tag{5}$$

The calculated error is distributed throughout the network on the backward path from the output layer through the network layers. In fact, the training algorithm tries to change the network weights in accordance with the following equation so that the sum of squared network errors can be minimized. The value of $\Delta W(s)$ is defined as:

$$\Delta W(s) = -\alpha \frac{\partial E}{\partial W(s)} + \beta \Delta W(s-1) \tag{6}$$

In the above equation, α and β are constants with values between zero and one, and they control the learning rate and the partial changes in the network weight respectively. Furthermore, *E* indicates the error function, *W* is the weight vector, and *s* is an index showing the number of iterations. Different algorithms can be used to train the network. With due regard of the previous studies, the authors used the Levenberg-Marquardt algorithm (LMA) in this study[8,15].

3.1 Feature extraction of data

It is difficult to extract the quantitative and qualitative features of an incremental nonlinear dynamic analysis curve, which also considers the characteristics of the earthquake as well as the structure. Due to the incremental procedure of IDA analysis, the extracted features do not have any specific distribution. On the other hand, each one of the earthquake features, such as Arias Intensity (IA), Cumulative Absolute Velocity (CAV), Characteristic intensity (IC) and specific energy density (SED) IMs, have a different range, which must be taken into consideration [8,15]. One of the most important and most common and basic assumptions in statistics is that the data is normal. Therefore, it must be ensured whether the data with this specific distribution can be used. More accurate results can be achieved by assigning appropriate distribution.

3.1.1 Feature extraction of ground motion data

Too much features is required for a complete description of strong ground motions. The selection of a ground motion intensity measure (IM) is very important to provide a probabilistic relationship between the ground motion hazard and the resulting seismic response of structures. Several studies have utilized the effects of using different IMs for Probabilistic Seismic Demand Models(PSDMs) analysis of structures such as the peak ground acceleration (PGA), the peak ground velocity (PGV), the damped spectral acceleration at the structure's fundamental- mode period (SA(T1, 5%)) with ξ = 5%. IA, IC, CAV and SED IMs are indicative the amplitude, the duration, the frequency content and energy of a strong ground motion, respectively [8,15]. Arias Intensity was expressed as a parameter related to the amplitude of the ground motion that indicate the potential damage of an earthquake as the time-integral of the square of the ground Acceleration :

$$I_A = \frac{\pi}{2g} \int_0^{\infty} [a(t)]^2 dt \tag{7}$$

Where g is the acceleration due to gravity (9.81 m/s2), a(t) is the acceleration time history. Then I_A is determined in units of velocity. The CAV is included a complex index of strong ground motion damage ability and is estimated as an area under absolute accelerogram According to the following equation :

$$\mathrm{CAV} = \int_0^{T_d} |a(t)| dt \tag{8}$$

Where a(t) is an absolute acceleration value in bracket duration(T_d) between the first and last exceedances of some threshold acceleration. The threshold acceleration level is usually 0.05g.

The types of spectra such as fourier spectra, power spectra or response spectra can be described of ground motion frequency content. Spectral parameters can be used in the form of dominant frequency, mean frequency, bandwidth, central frequency, etc. However, the I_C is defined as follows :

$$I_C = a_{rms}^{1.5} T_d^{0.5} \tag{9}$$

Root mean square (RMS) acceleration ground motion parameter is defined as a_{rms}. SED is obtained by integrating velocity square over effective duration of an earthquake and has units of m2/s. This parameter captures the variation in kinetic energy input during T_d and is defined in equation 10 :

$$SED = \int_0^{T_d} [v(t)]^2 dt \tag{10}$$

Hence, in order to establish a appropriate estimation of the seismic performance of the structure, a set of corrected strong ground motion records have been collected [16]. The strong ground motion data includes all types of soil, magnitudes (ML) ranging from 4.5 to 7.5, closest distance to the surface projection of the fault plane in the range of 20 to 70 km and types of faults. Fig. 2 presents acceleration response spectra of ground motions.

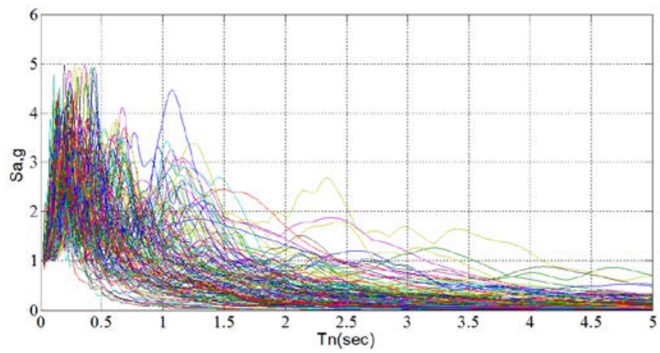

Fig. 2 – Earthquake acceleration response spectra including 129 records

3.1.2 Feature extraction of NTHA outputs

Similarly, response selection (targets) from NTHA analysis in NN is used as target values. Responses are also included in maximume piers ductility and maximume abutment diformations. The reason for selecting piers ductility is due to the superstructure is expected to remain linearly elastic under seismic loading. Obviously, the stability of the bridge is depended to the piers.

4. Fragility curves based on neural network results

IDA is provided a comprehensive assessment of maximum response of structure, sometimes called engineering demand parameter (EDP) versus appropriate intensity measure(IM) which is chosen to represent the seismic hazard (e.g. PGA, Sa). As it mentioned ANN model is a computational model that is inspired by the structure and the functionality of biological neurons. It is used as nonlinear statistical data modeling tool to model complex relationships between inputs and targets. As mentioned previously, ANNs are useful in applications where the underlying process is complex, such as nonlinear response estimation of structures. Therefore, the prediction of the seismic demand of structure based on NN for a limit state, Architecture and network training is very important. Obviously, the ability to predict neural network is dependent to input parameters such as IA, IC , CAV and SED which representative of earthquake ground motions.

4.1 Description of example bridge and numerical simulation

To demonstrate the development of analytical fragility curves, the three-Span Continuous Curved Steel Girder Bridge is used, which have the most abundant of the bridge in terms of the number of spans. The typical bridge configuration used in this study has three spans which all have the same length of 30.3 m giving an overall length of 90.9 m to the bridge and the height is 5.2m. The bridge structure created in OpenSees. The detailing for

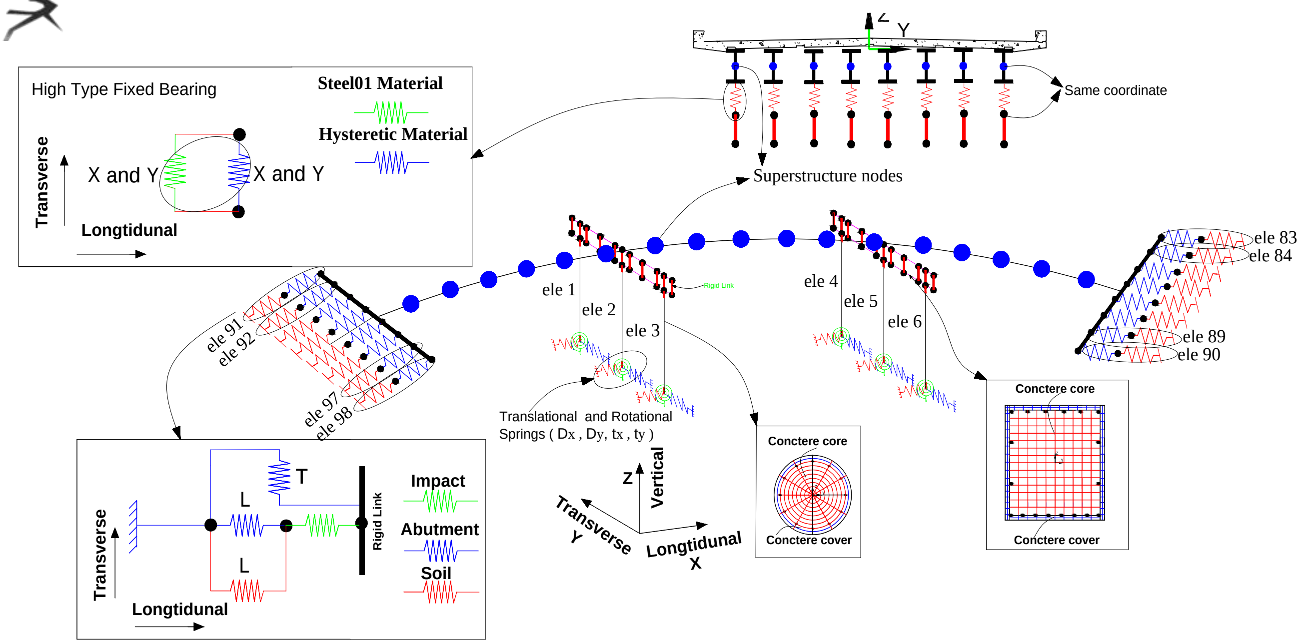

the typical reinforced concrete column, the discretization of beam and cross-sections of the superstructure shows in Figure 3. When the superstructures are made continuous, the demand appears to shift partially from the bearings to the columns and abutments. The deck are modeled using elastic beam-column elements. The deck width for this bridge is also 15 m and constructed with eight steel plate girders. The bearing model considers high type bearings, that is typically used for longer spans and therefore deemed appropriate for this model. The nominal cylindrical strength for the concrete is assumed to be 20.7 MPa while nominal yield stress of reinforcing steel has a yield strength of 414 MPa. The unconfined concrete behavior of column and cap beam sections is modeled using the Concrete01 material as provided in OpenSees. This material uses the Kent-Scott-Park model which utilizes a degraded linear uploading-reloading stiffness and a residual stress. The elements for the columns and cap beams are generated using displacement beam-column elements in OpenSees that have an associated fiber section being representative of the true column section. The bridges use a 914.4 mm diameter circular column with 12 28.58mmϕ bars. It should be noted that the curvature of the bridge is 45 degrees, which is similar straight bridges can be analyzed [17] .

Fig. 3 –Finite element model of horizontal steel curved bridge

4.2 Statistical analysis of the distribution of inputs

Analysis of the input data has shown that the input variables does not have a specific distribution. There are a number of methods that make some changes to data in order to normalize them. The log transform, the Box-Cox transform, the log probability plot, Finney plot, and etc. are some of the available normalization methods. It was observed the results of Box-Cox transform do not fall into an acceptable range for kurtosis and skewness, and therefore, the normality hypothesis is rejected. In Log transform method, Let x_i be a variable, then the following transform is applied :

$$y = Ln(ax_i \pm b) \tag{11}$$

Where *a* is usually set to 1 and *b* has a positive or negative value.

As it is shown in tables 1 and 2, the kurtosis and skewness values indicate that the normality hypothesis is confirmed. Also, the Kolmogorov-Smirnov and Shapiro-Wilk tests both confirm the normality of the data after applying this transform. The appropriate normal distribution fitted to each of the earthquake features, after applying the log transform. The linear formation of the data on Q-Q plot and the appropriate range of data in box plot, after applying the log transform (the finalized input data of the neural network) is shown in figure 4 for Arias Intensity.

4.3 NN predictions sheme

When using neural networks to perform predictive modeling, the input layer contains all of the input fields or variables used to predict the outcome variable. In this section the prediction capabilities of the trained NN for two damage measure has been investigated. The objective of the NN prediction scheme is to estimate the EDP for various combinations of the four IMs that are represented reliable of the ground motions.

Table 1 –Transformed data

		Iax	**Icx**	**SEDx**	**CAVx**	**Iay**	**Icy**	**SEDy**	**CAVy**
N	**Valid**	129	129	129	129	129	129	129	129
	Missing	0	0	0	0	0	0	0	0
Mean		-2.13	-4.54	4.37	5.7	-2.09	-4.51	4.39	5.73
Skewness		-0.22	-0.43	-0.2	-0.31	-0.08	0.01	-0.17	-0.29
Std. Error of Skewness		0.22	0.22	0.22	0.22	0.22	0.22	0.22	0.22
Kurtosis		0.40	1.93	0.24	0.13	-0.05	-0.36	0.23	0.40
Std. Error of Kurtosis		0.44	0.44	0.44	0.44	0.44	0.44	0.44	0.44

Table 2 – Tests of Normality

Transformed data	**Kolmogorov-Smirnov**			**Shapiro-Wilk**		
	Statistic	**df**	**Sig.**	**Statistic**	**df**	**Sig.**
IAx	0.049	129	0.200	0.993	129	0.838
ICx	0.046	129	0.200	0.976	129	0.032
SEDx	0.054	129	0.200	0.991	129	0.599
CAVx	0.074	129	0.16	0.988	129	0.39
IAyx	0.05	129	0.200	0.994	129	0.872
ICy	0.056	129	0.200	0.992	129	0.684
SEDy	0.058	129	0.200	0.991	129	0.628
CAVy	0.067	129	0.200	0.984	129	0.168

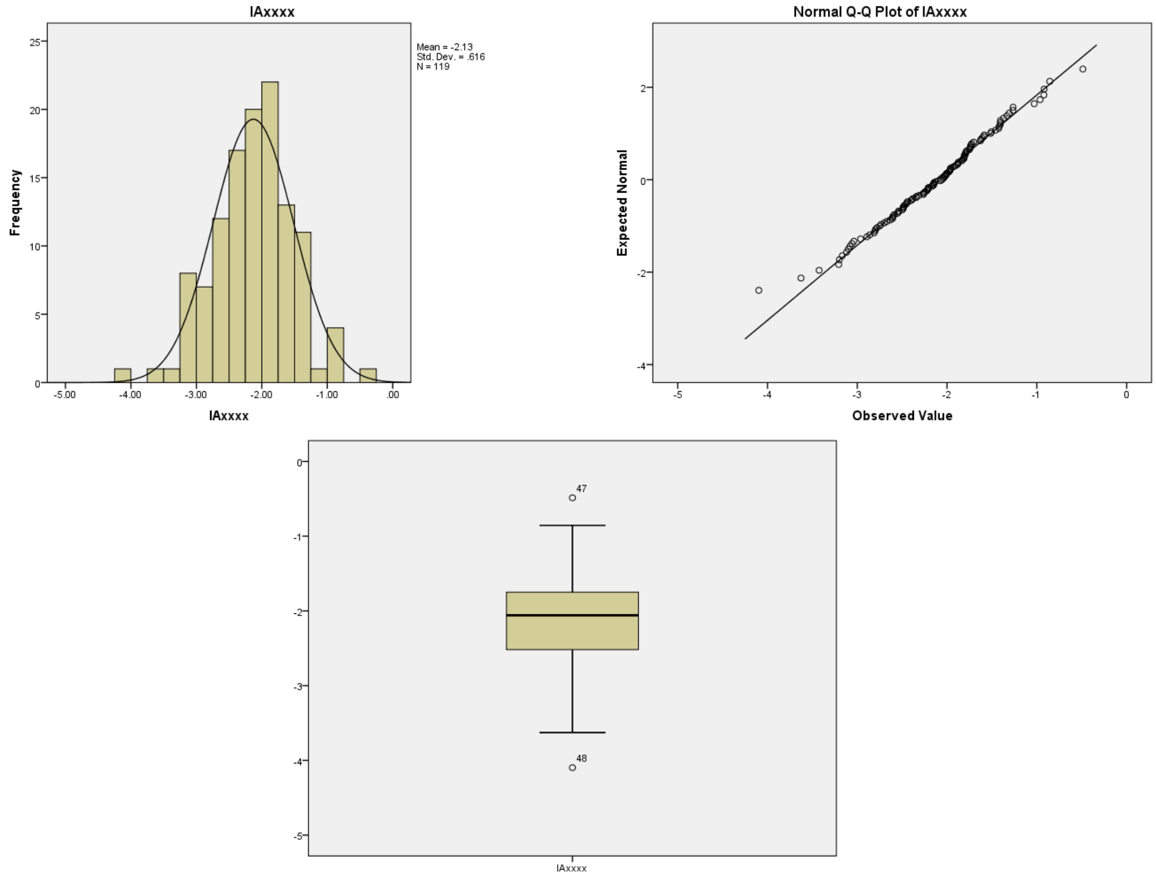

Fig. 4 –Normalized, Q-Q and box plot of data (e.g Arias Intensity)

Therefore, the number of input nodes of the NN is 4 with two hidden layers and hidden nodes which provides a compatibility between accurate predictions and computationally efficient calculations. The output layer has 4 nodes corresponding to the EDP for the IMs. Thus, all processes performed up to this section is illistrated in Fig.5.

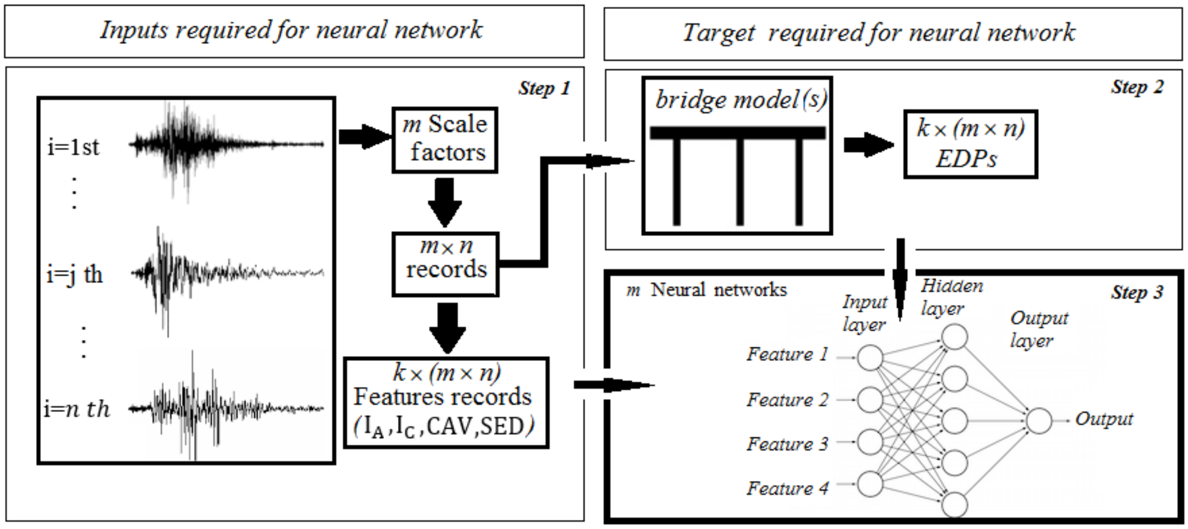

Fig. 5 – Neural network based incremental dynamic analysis

In the other words, the trend of using inputs and outputs data of the neural network is shown in the recent figure. Feedforward networks with tan-sigmoid transfer function in the hidden layer and linear transfer function in the output layer is used. This type of neural networks associated with the applications are estimates of regression functions efficiently. By trial and error out of 10 neurons in the hidden layer was determined. Figure

6 represent the regression plot, histograms error and mean square error. The results of analyzing the time history of 129 earthquakes and the neural network predictions (ductility measure of piers in fragility curves) are represented in 13 seismic groups with the same PGAs.

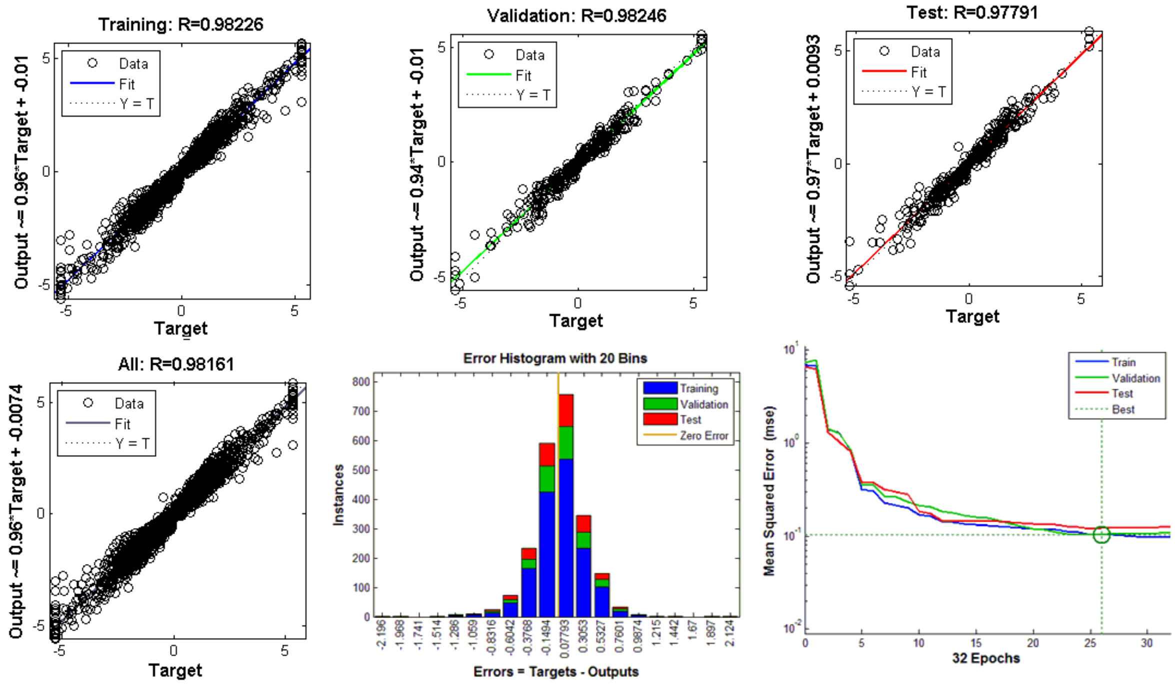

Fig. 6 –Regression plot, histograms error and mean square error for pier ductility

5. Results

Two approaches are used for prediction. In the first approach, the prediction is performed within each one of the seismic groups (by increasing the PGA). 129 samples, extracted from the nonlinear dynamic analysis, are used in each one of the seismic groups. Firstly, in the second approach, the prediction is performed in a seismic group that contains all the input data from the previous 13 seismic groups. Despite having 1677 samples in recent approach, the evaluation results of the neural network with 4 outputs such as absolute maximum pier ductility in two directions showed low accuracy. Because of the incremental procedure of adding inputs and outputs, the data does not follow a proper distribution, and thus causes more complexities for the neural network. Therefore, for prediction in the second approach the outputs are computed separately and 4 neural networks are used. Average predicted results show more than 85 percent accuracy in regression (Table 3, 4). Fig 6 and 7 demonstrated the fragility curves at each different limit state based on NN and NTHA methods. The results obtained using the NN method are compared with those obtained by the conventional method of NTHA, In the first approach it was found that the probability of failure on extensive and collapse situation under-estimated the seismic fragilities while the second approach shows little difference in high seismic intensity. Approach

Table 3 – Prediction of response structure by NN in thirteen seismic scale, in training, validation and testing steps for curvature ductility (Approach 1)

seismic scale(PGA)	Training			Validatin with training			Testing		
		Results from NN			Results from NN			Results from NN	
		R	Equation		*R*	Equation		*R*	Equation

0.1g		R=0.94	Y= 0.86*Target + 0.00098		R=0.95	Y=1*Target - 0.005		R=0.94	Y=0.91*Target + 0.0028
0.2g		R=0.94	Y= 0.87*Target + 0.0026		R=0.96	Y= 0.94*Target + 0.01		R=0.92	Y= 0.94*Target + 0.0023
0.3g		R=0.96	Y= 0.94*Target + 0.0031		R=0.83	Y= 0.95*Target + 0.013		R=0.91	Y= 0.74*Target + 0.027
0.4g		R=0.95	Y= 0.91*Target + 0.0009		R=0.94	Y= 0.84*Target - 0.035		R=0.94	Y= 0.77*Target + 0.0058
0.5g		R=0.95	Y= 0.98*Target - 0.028		R=0.91	Y= 0.94*Target - 0.074		R=0.89	Y= 0.91*Target - 0.023
0.6g		R=0.95	Y= 0.84*Target + 0.016		R=0.9	Y= 0.93*Target + 0.021		R=0.95	Y= 0.9*Target + 0.034
0.7g		R=0.95	Y= 0.84*Target + 0.0098		R=0.90	Y= 0.85*Target + 0.032		R=0.93	Y= 0.9*Target + 0.0099
0.8g		R=0.94	Y= 0.93*Target - 0.21		R=0.93	Y= 0.88*Target - 0.098		R=0.92	Y= 0.93*Target - 0.19
0.9g		R=0.93	Y= 0.83*Target + 0.036		R=0.90	Y= 0.96*Target + 0.15		R=0.91	Y= 0.89*Target + 0.18
1g		R=0.92	Y= 0.84*Target - 0.013		R=0.95	Y= 0.89*Target -0.041		R=0.92	Y= 0.78*Target + 0.03
1.1g		R=0.95	Y= 0.86*Target + 0.04		R=0.94	Y= 0.86*Target + 0.22		R=0.89	Y= 0.89*Target + 0.16
1.2g		R=0.97	Y= 0.94*Target + 0.0046		R=0.95	Y= 0.87*Target + 0.13		R=0.95	Y= 0.94*Target - 0.12
1.3g		R=0.96	Y= 0.83*Target - 0.17		R=0.91	Y= 0.95*Target - 0.1		R=0.91	Y= 0.88*Target - 0.0081

Table 4 – Prediction of response structure by NN in a in a seismic data set, in training, validation and testing steps for curvature ductility (Approach 2)

For all imputs	Training			Validatin with training			Testing		
		Results from NN			Results from NN			Results from NN	
		R	Equation		*R*	Equation		*R*	Equation
Response-XP		R=0.98	Y=0.97*Target + 0.054		R=0.97	Y=0.96*Target + 0.064		R=0.95	Y=0.98*Target + 0.058
Response-XN		R=0.98	Y=0.96*Target - 0.057		R=0.96	Y=0.93*Target-0.11		R=0.97	Y=0.96*Target -0.078
Response-YP		R=0.98	Y=0.95*Target + 0.064		R=0.95	Y=0.91*Target + 0.11		R=0.94	Y=0.91*Target + 0.13
Response-YN		R=0.97	Y=0.95*Target - 0.073		R=0.95	Y=0.89*Target -0.14		R=0.95	Y=0.91*Target - 0.081

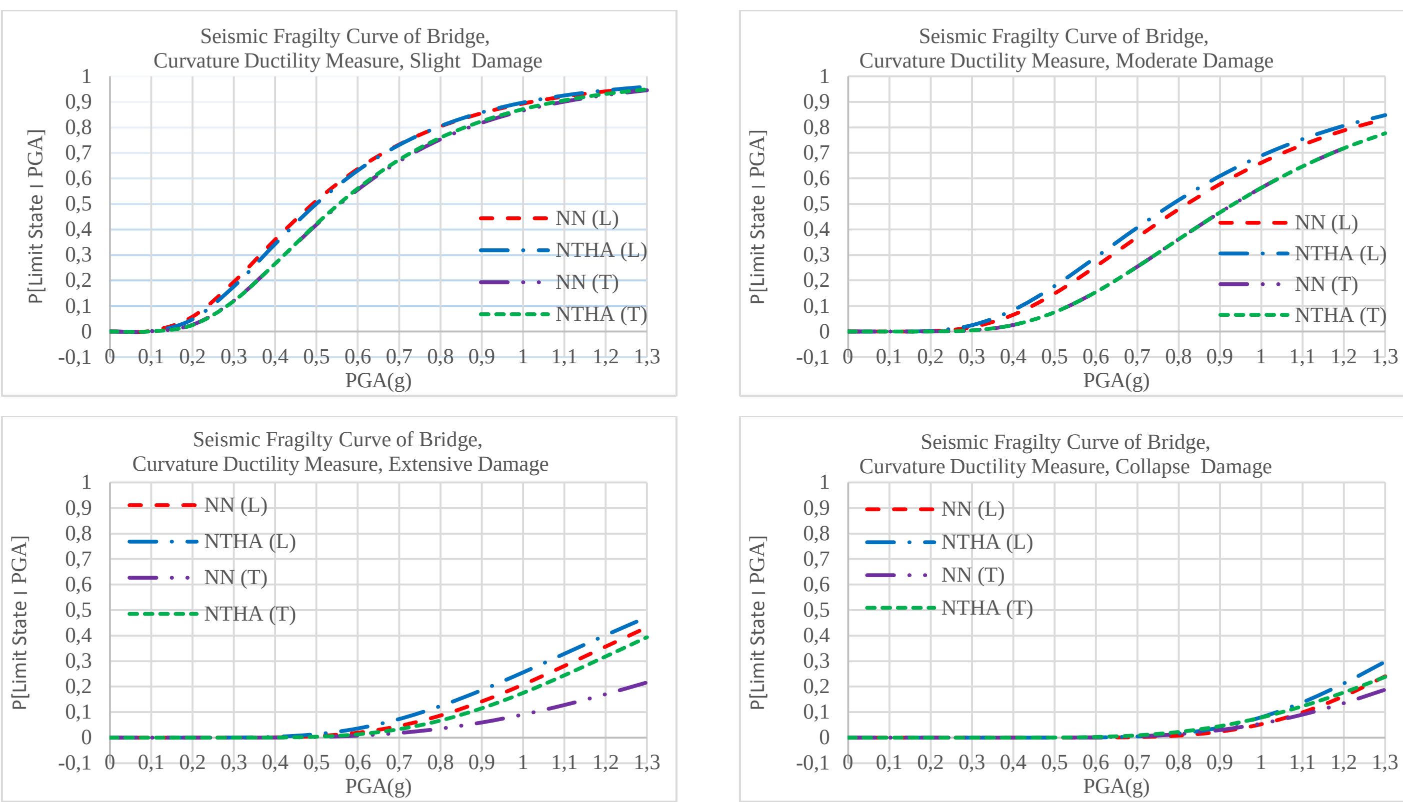

Fig. 7 –Comparison of the fragility curves by NN (Approach 1) and NTHA methods

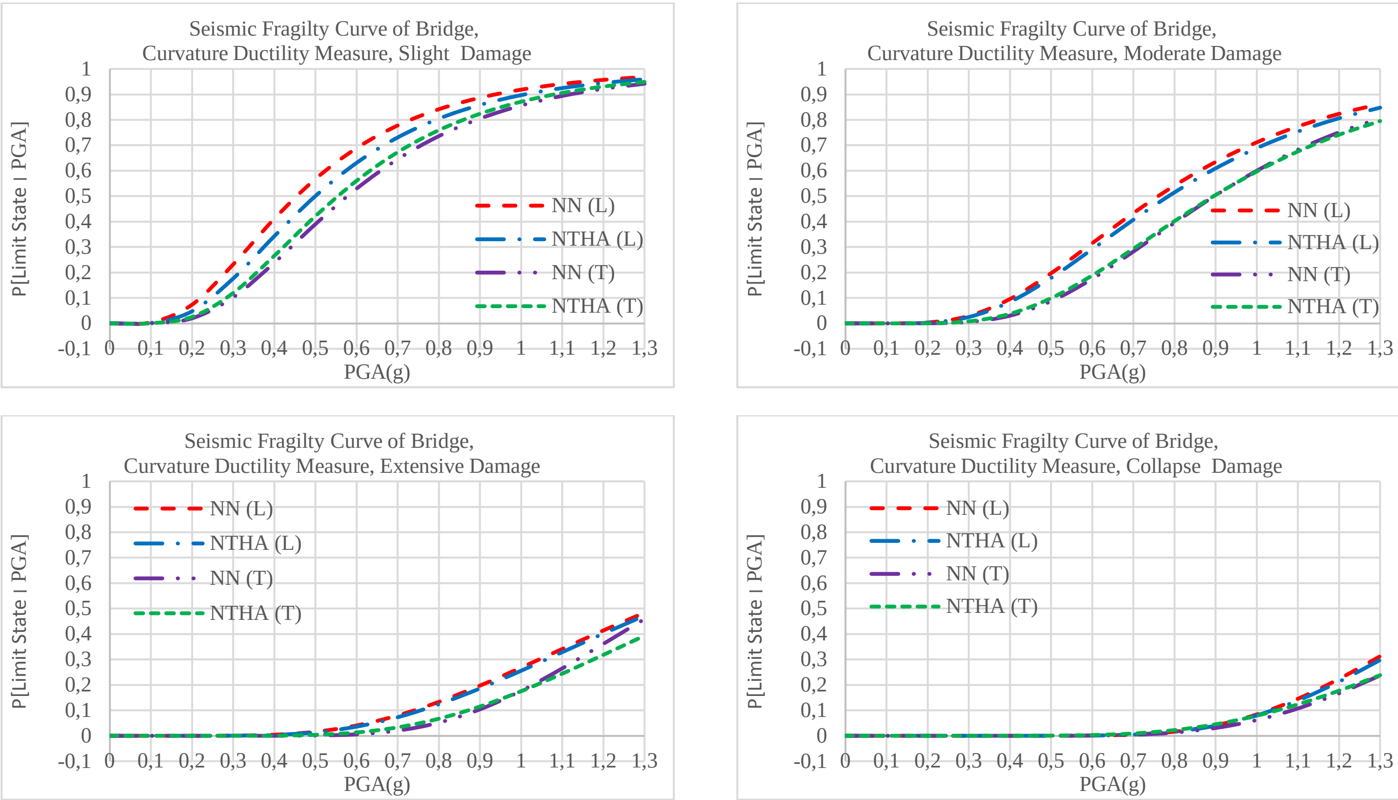

Fig. 8 –Comparison of the fragility curves by NN(Approach 2) and NTHA methods

6. Conclusion

The primary objective of this study was to achieve seismic fragility curves of the structure using "Soft Computing based framework" tools and to compare analytically seismic fragility approach. Indeed, the proposal of a new approach based fragility evaluation is the most significant highlight. Comparing the fragility curves of the neural network and time history analysis shows that the curves have proper compliance in two directions. In both of the approaches, the difference of these curves is reasonable from slight to collapse limit states; which considering the non linearity and complexity of the problem that must be solved by the neural network. The only significant difference of probability of failure between the curves is due to the range of damage index and the coefficients of linear equations fitted in the neural network. Obviously, the number of training samples increases, it becomes more functionality and efficiency of the network. Note that the curves for the second approach have a better performance in high seismic intensity. In future research, for a structural benchmark, its main advantage is the reduction of time in the extraction of fragility curves by applying NN. The fragility curves based approach discussed here can be extended to include uncertainties, the reliability of the neural network and accuracy remain potential issues for investigation.

7. References

[1] Mander J, (2000): Fragility curve development for assessing the seismic vulnerability of highway bridge. *University at Buffalo, State University of New York.*

[2] Kim SH, Feng MQ (2003): Fragility analysis of bridges under ground motion with spatial variation, *International Journal of Non-Linear Mechanics* **38**, 705 – 721.

[3] Rezaul Karim K, Yamazaki F (2007): Effect of isolation on fragility curves of highway bridges based on simplified approach. *Soil Dynamics and Earthquake Engineering*, **27**, 414–426.

[4] Kim SH, Shinozuka M, (2007): Development of fragility curves of bridges retrofitted by column jacketing. *Probabilistic Engineering Mechanics* **19** (2004) 105–112.

[5] Nielson B (2005): Analytical Fragility Curves for Highway Bridges in Moderate Seismic Zones, *A Thesis a presented to the Academic Faculty*.

[6] Padgett, JE. and DesRoches, R (2007): Sensitivity of Seismic Response and Fragility to Parameter Uncertainty. *Journal of Structural Engineering*, (ASCE) **133** (12), 0733-9445.

[7] Carlo Marano G, Greco R, Morronea E, (2011): Analytical evaluation of essential facilities fragility curves by using a stochastic approach. *Engineering Structures* **33**(2011), 191–201.

[8] Mitropoulou CC,Papadrakakis M, (2011): Developing fragility curves based on neural network IDA predictions. *Engineering Structures* **33** (2011) 3409–3421.

[9] Rajeev P, Tesfamariam S, R (2012): Seismic fragilities for reinforced concrete buildings with consideration of irregularities. *Structural Safety* **39** (2012) 1–13.

[10] Penna A,Rota M, Mouyiannou M, Graziotti F, Magenes G (2013): An analytical procedure for the derivation of state-dependent fragility curves for masonry buildings. Recent Advances in Earthquake Engineering and Structural Dynamics 2013 (*VEESD 2013*).

[11] Goda K, Yoshikawa H (2013): Incremental dynamic analysis of wood-frame houses in Canada: Effects of dominant earthquake scenarios on seismic fragility. *Soil Dynamics and Earthquake Engineering.* **48** (2013) 1–14.

[12] Hancilar U, Çaktı E, Erdik M, Franco G ,Deodatis G (2014): Earthquake vulnerability of school buildings: Probabilistic structural fragility analyses. *Soil Dynamics and Earthquake Engineering* **67**(2014)169–178.

[13] Siqueira GH, Sanda AS,Paultre P, Padgett JE (2014): Fragility curves for isolated bridges in eastern Canada using experimental results. Engineering Structures **74** (2014) 311–324.

[14] Walter Yang CH, Werner SD, DesRoches R (2015): Seismic fragility analysis of skewed bridges in the central southeastern United States, Engineering Structures **83** (2015) 116–128.

[15] Lagarosa ND, Fragiadakisa M (2007): Fragility Assessment of Steel Frames Using Neural Networks. *Earthquake Spectra*, **23**, No. 4, pages 735–752.

[16] PEER ground motion database.

[17] Open System for Earthquake Engineering Simulation (OpenSees).